Synchronous removal of Cd(II), Pb(II), and Cu(II) by coagulation in the presence of polymeric ferric sulfate

Chengyu Suo[a,†], Dandan Xu[b,†], Rongfang Yuan[a,*], Beihai Zhou[a,*]

[a]*Beijing Key Laboratory of Resource-oriented Treatment of Industrial Pollutants, School of Energy and Environmental Engineering, University of Science and Technology Beijing, Beijing 100083, China, emails: yuanrongfang@ustb.edu.cn (R. Yuan), zhoubeihai@sina.com (B. Zhou), 1142728357@qq.com (C. Suo)*
[b]*Rural Energy and Environmental Agency, Ministry of Agriculture and Rural Affairs, Beijing 100125, China, email: xddustb2016@163.com (D. Xu)*

ABSTRACT

In this research, polymeric ferric sulfate (PFS) was used as a coagulant to treat wastewater containing Cd(II), Pb(II), and Cu(II). Based on a large number of single-factor experiments, response surface methodology (RSM) with Box–Behnken design (BBD) was employed to investigate the effects of PFS dosage, pH value, and precipitation time on the removal efficiencies of these heavy metals, and a quadratic polynomial response surface model was established. The result for the analysis of variance (ANOVA) shows that the significant order of these factors was as follows: pH > PFS dosage > precipitation time. The optimum PFS dosage, pH value, and precipitation time were found to be 59.6 mg/L, 8.04, 45.4 min for coagulation experiment in the combined heavy metals wastewater with the concentration of Cd(II), Pb(II) and Cu(II) of 5, 50, and 25 mg/L, 50 times of the requirement of the "Integrated Wastewater Discharge Standard of China" (GB 8978-1996), respectively. The remaining concentrations of combined heavy metals in both pure water and real wastewater could all reach the "Integrated Wastewater Discharge Standard in China" (GB 8978-1996). Meanwhile, the zeta potential of the supernatant and the fractal dimension (D_f) of the flocs after precipitation under the optimal coagulation conditions were measured to illustrate the consistency of the removal efficiency of heavy metals with the trend of zeta potential and fractal dimension. The electric neutralization and purge coagulation play a relatively dominant role in the coagulation of heavy metals in aqueous solution.

Keywords: Polymeric ferric sulfate; Response surface methodology; Coagulation; Combined heavy metals; Fractal dimension

1. Introduction

With the development of automobile manufacturing, electronics, petrochemical, and other industries, wastewater containing various heavy metals was discharged into the environment increasingly [1,2]. The typical heavy metals in the discharged wastewater, such as Cd(II), Pb(II), and Cu(II), have aroused high attention due to their toxicity and carcinogenicity. The heavy metals could transfer into the human body through food chains, leading to extremely serious consequences [3,4]. In addition, the adverse effects are strengthened if the metals are combined [5]. Therefore, it is necessary to remove combined heavy metals from aqueous solutions efficiently.

Generally, several technologies, including coagulation, ion exchange, chemical precipitation, adsorption [6,7], electric treatment, and biosorption [8,9], have been used for the removal of heavy metals. Among these technologies, the

---

* Corresponding author.

†These authors have contributed equally to this work and should be considered as the co-first authors.

electric treatment is always covering a small area, whereas it has large power consumption and the wastewater treatment capacity is too small. The chemical precipitation method is widely applied due to its simplified equipment, low investment, and convenience of operation; however, its treatment process is too long, and a large amount of sludge are often produced [10]. Adsorption method is efficient, but the adsorbents used in this process are expensive. Heavy metals can be recovered by ion-exchange without secondary contamination, but the resin is susceptible to contamination. Compared to the other treatments, enhanced coagulation requires lower capital cost, and is effective for heavy metals removal [11,23].

In general, inorganic salt coagulants including $FeCl_3$ [12], $FeSO_4$, and $Al_2(SO_4)_3 \cdot 18H_2O$ [13], as well as the high polymer coagulants such as poly aluminum chloride, polymeric ferric sulfate (PFS) [14] and poly aluminum ferric chloride, have been widely used in the removal of heavy metals by coagulation. Among these coagulants, PFS is more preferred as it had lower residual Fe concentrations and better coagulation effect than other coagulants. The Fe in PFS was a transition metal ion with strong deformability which exhibited stronger polarization ability than other coagulants and thus produced a strong bond with the heavy metal ions [15]. However, sometimes the formation of the flocs is too slow, and coagulant aid is often added to promote the precipitation process. In this study, polyacrylamide (PAM) was chosen as the coagulant aid for its good coagulation effect and shear resistance.

The coagulation efficiency was affected by the species and dosage of coagulant, the value of pH, the precipitation time, or other variables [16,17]. Recent researches were focused on single variable experiments, whereas the interaction between the different factors has been neglected [18]. Response surface methodology (RSM) is an efficient and logical scheme design approach matching mathematics and statistics organically to model, improve, and optimize the multi-factor experiments [19,20]. RSM could be used in the sensitivity analysis of various measures for different kinds of random graphs and errors [21]. Identifying and fitting an appropriate response surface model from experimental data requires some use of statistical experimental design fundamentals, regression modeling techniques, and optimization methods [22]. Box–Behnken design (BBD) can evaluate the nonlinear effects of the factors without as many tests as other approaches [23]. Therefore, RSM combined with BBD were used in this study. In addition, at present, most studies have been focused on the coagulation and precipitation of single heavy metal, but few studies on complex heavy metals.

In this study, the influences of the parameters including PFS dosage, pH value, and precipitation time on the removal rates of Cd(II), Pb(II), and Cu(II) were investigated by single-factor experiments. Then, the abovementioned parameters were optimized by RSM, and the interaction between the factors was revealed. Under the condition of optimal parameters, the coagulation experiments in pure water and real wastewater added with heavy metals were carried out to investigate whether the effluent meets the "Integrated Wastewater Discharge Standard of China" (GB 8978-1996). In addition, the mechanism of coagulation was explained by the aid of some characterizations.

2. Materials and methods

2.1. Materials

$Cd(NO_3)_2 \cdot 4H_2O$, $Pb(NO_3)_2$, and $Cu(NO_3)_2 \cdot 3H_2O$ (analytical grade), which were purchased from Sinopharm Shanghai Testing Co., Ltd., (Shanghai, China), were used to prepare the solution containing heavy metals. PFS (>19%, based on Fe element) and PAM (molecular of 22–25 million), purchased from Beihua Fine Chemicals Co., Ltd., (Beijing, China), were used as coagulant and coagulant aid, respectively. The deionized (DI) water used in this study was obtained from Milli-Q water purification system (Millipore Synergy 185, US). The initial concentrations of Cd(II), Pb(II), and Cu(II) in the single or combined water samples were 5, 50, and 25, respectively (50 times of the value in the "Integrated Wastewater Discharge standard of China"). Then, the above three heavy metals were added into the influent of Shengke Wastewater Treatment Plant in Tianjin. The water quality parameters are shown in Table 1.

2.2. Coagulation tests

The coagulation tests were carried out in 1 L beakers with the help of a mixer (MY3000-6N, Meiyu, China). Single-factor tests were conducted to provide the range of the values for the parameters before response surface experiments. The initial pH was adjusted to 3.0–11.0 using 1.0 mol/L HNO_3 or NaOH solutions, and PFS with a dosage of 0.5–30.0 mg/L was added. The samples were rapidly mixed by stirring at 250 rpm for 1.5 min, followed by an intermediate mix at 100 rpm for 3.0 min. Then, the solution was stirred at 40 rpm for 3.5 min in the presence of 1 g/L PAM. After precipitation for 30 min, the supernatant was taken out and filtered through a 0.45 μm membrane (Millipore, Livingston, UK) before measuring the heavy metal concentration and the zeta potential of the samples.

Based on the results of the single factor tests, the response surface optimization experiments with a 3-factor and 3-level BBD was conducted. Three variables including PFS dosage (5–65 mg/L, X_1), pH (3.0–9.0, X_2), and precipitation time (10–70 min, X_3), as well as the removal efficiencies (Y) of Cd(II), Pb(II), and Cu(II) were considered. These factors selected above were investigated at high (+1), middle (0),

Table 1
Real sewage water quality parameters

Index	Value (mg/L except pH)
COD	260
TN	72
TP	2.5
NH_3–N	40
pH	7.5
SS	48
Cd	5
Cu	25
Pb	50

and low (–1) (Table 2). The variables were coded according to Eq. (1):

$$x_i = \frac{\left(X_i - X_0\right)}{\Delta X} \tag{1}$$

where x_i is the variable coded value, X_i is the true value of the variable, X_0 is the true value of the variable at the test center point, and ΔX is the change step size of the variable [24].

Design expert software version 10.0.3 was used for the design and optimization of the experiments, and a regression quadratic polynomial model was proposed as Eq. (2) [25,26]:

$$Y = \beta_0 + \sum_i^k \beta_i X_i + \sum_i^k \beta_{ii} X_i^2 + \sum_{i<j}^k \beta_{ij} X_i X_j + \varepsilon \tag{2}$$

where Y is the predicted response value, β_0 is the intercept state, β_i $(i = 1,2, …, k)$ is the linear coefficient, β_i $(i = 1,2, …, k)$ is the squared coefficient, β_{ij} $(i = 1,2, …, k, j = 1,2, …, k)$ is the interaction coefficient, X_i, X_j, …, X_k indicate the independent variables, and ε represents the random error.

2.3. Analytic methods

The concentration of target metals (Cd(II), Pb(II), and Cu(II)) were measured with an Optima 8300 inductively coupled plasma emission spectrometer (ICP-OES, Beaconsfield, UK). An HQ11d pH meter (Hach, USA) was used for pH measurement. Zeta potential was analyzed with a Zetasizer Nano ZS90 (Malvern, UK)

The scanning electron microscopy (SEM) images of the flocs were acquired with a Zeiss Evo 18 electron microscope (German). The flocs images (×250) were obtained with an E-250 digital camera (OLYMPUS, Japan). The composition and surface chemical state of flocs were characterized via the X-ray photoelectron spectroscopy (XPS, Thermo Fisher Scientific, US). The projected area (A) and perimeter of the flocs (P) were measured by Image Pro Plus (IPP) software, and the two dimensional fractal dimension (D_f) of the flocs were obtained from Eq. (3) [27]:

$$\ln A = D_f \ln P + \ln Y \tag{3}$$

where P is the perimeter of the flocs, A is the projection area of the flocs, and Y is a constant.

3. Results and discussion

3.1. Coagulation of single heavy metal in DI water

3.1.1. Effect of PFS dosage

The optimization experiments of PFS dosage was carried out with the initial concentrations of Cd(II), Pb(II), and Cu(II) of 5, 50, and 25 mg/L, respectively. The initial pH of the water sample was set at 9.0, and the precipitation time was 30 min (Fig. 1).

It can be seen from Fig. 1a that the removal efficiency of Pb(II) increased gradually and obtained a maximum

Table 2
Factor levels and code of Box–Behnken experimental design

Variable	Symbols	Levels		
		–1	0	1
PFS dosage (mg/L)	X_1	5	35	65
Initial pH	X_2	3	6	9
Precipitation time (min)	X_3	10	40	70

at a dosage of 15 mg/L after which the removal efficiency showed no significant increase. Moreover, the optimum dosage for Cd(II) and Cu(II) were approximately 30 and 3.0 mg/L, respectively. When the dosage was relatively low, the metal hydroxides could not be coagulated into large flocs and then settled. The supernatant was suspended with bits of very small flocs which were difficult to precipitate [26]. Fig. 1b shows that better coagulation effect could be obtained when the absolute value of the zeta potential of the water sample was close to zero [28].

The D_f of the flocs reflects the surface morphology and compactness of the flocs [29]. It was reported that the flocs with larger D_f showed stronger absorption attached bridging ability in the coagulation system, and thus the coagulation efficiency was enhanced. Fig. 1c showed that the D_f shared a similar trend as the removal efficiency vs. the dosage with the increase of the PFS dosage. If the PFS dosage continued to increasing, back mixing was occurred, resulting in the loose flocs and a decreased D_f.

3.1.2. Effect of initial pH

As presented in Fig. 2, the removal efficiency of Pb(II) ascended from 97.53% to 99.02% with the increasing pH from 3.0 to 6.0. This was due to the high hydrophobicity of the cross-linked hydride complexes, which could accelerate the coagulation reaction. However, there was no significant removal efficiency fluctuation when the pH value was increased from 6.0 to 8.0, and when the pH was 8.0–11.0, the Pb(II) removal rate was decreased because of the dissolution of the flocs. Therefore, pH 6.0–8.0 was chosen to be the optimum condition for the following experiments. Similarly, there were peak values for Cd(II) and Cd(II) removal at pH values of 6.0–7.0 and 9.0–10.0, respectively. The higher optimized pH for Cd(II) was obtained, and this can be explained as the higher K_{sp} (the solubility product) of $Cd(OH)_2$ when compared with those of the other two heavy metals.

In addition, as shown in Fig. 2b, the zeta potential values of the supernatants of the three heavy metals after coagulation and sedimentation under different pH conditions were determined. The results showed that when the pH was at 9.0–10.0, 6.0–8.0, and 6.0–7.0, the zeta potential of the supernatant containing Cd(II), Pb(II), and Cu(II) was closest to zero, which was in line with the variation trend of the removal efficiency of the three heavy metals as pH changed, indicating that the coagulation effect was the best at this time [30].

Experiments under different pH conditions were conducted and the relationship between removal efficiency
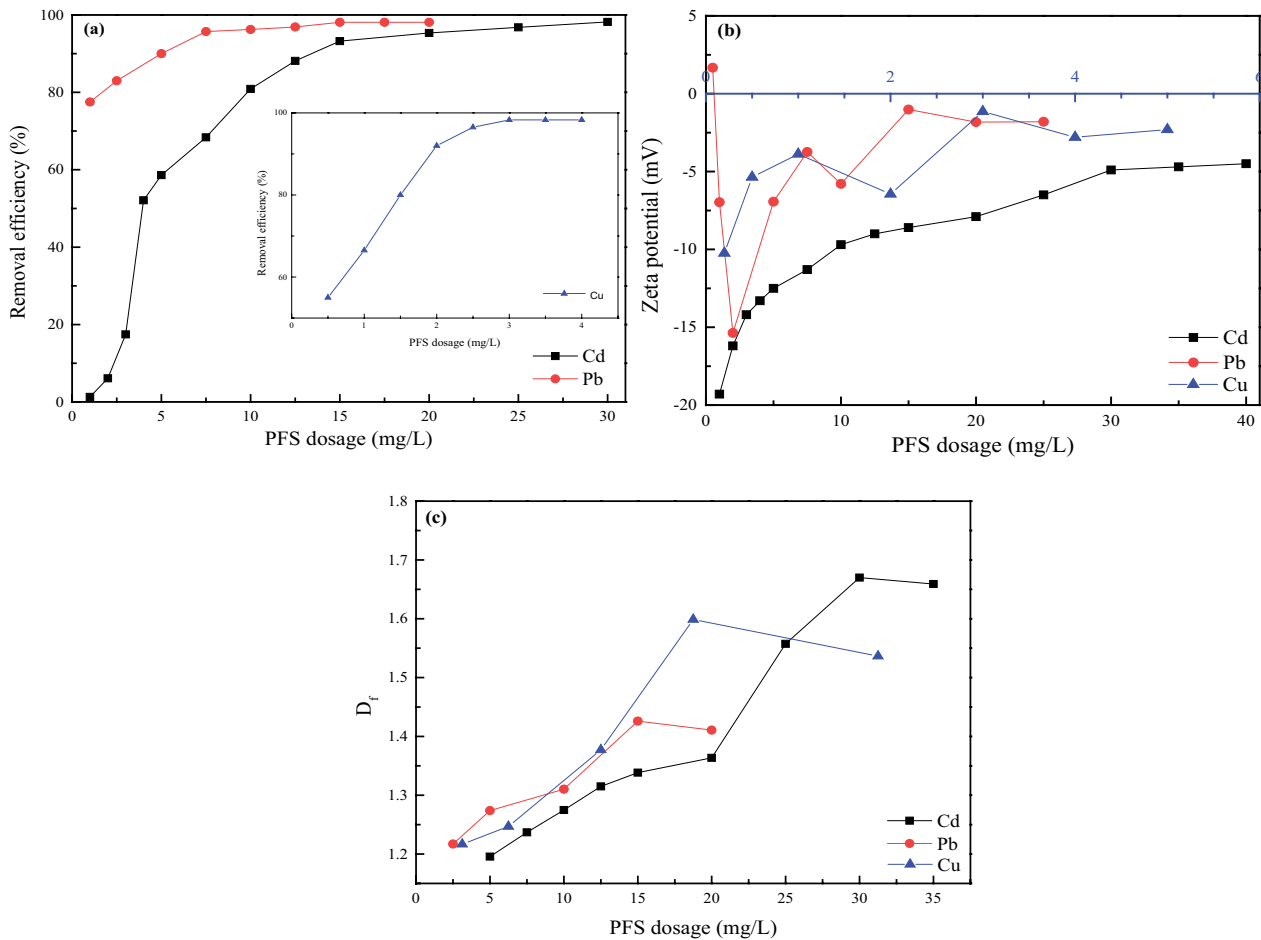
Fig. 1. Effect of PFS dosage on the coagulation of single heavy metals (a) removal efficiencies, (b) zeta potential, and (c) fractal dimension.

and the fractal dimension of flocs was then analyzed. As shown in Fig. 2c, the D_f of flocs showed a significant increase under neutral or slightly acidic condition, especially in the pH range of 5.0–6.0, and when the pH value was 9.0–10.0, 6.0–8.0, and 6.0–7.0 for Cd(II), Pb(II), and Cu(II), the D_f peaks of three heavy metals were achieved, and then decreased with the increase of pH value. Similarly, the removal efficiency of the three ions also shows a similar trend (Fig. 2a), demonstrating the credibility of the previously determined optimal pH condition. The coagulation mechanism and internal repulsion had an impact on the structure and morphology of flocs jointly, and it showed a lower repulsion which could promote the formation of the compact structure of flocs when pH was not too high. At this time, the charge neutralization and furl mechanism of PFS or other coagulant aid played the dominant role in the formation of flocs with a larger D_f under the selected optimal pH condition.

3.1.3. Effect of precipitation time

The effects of precipitation time on removal efficiencies of the heavy metals were investigated (Fig. 3), with the optimized values of pH value and PFS dosage were used.

As shown in Fig. 3, the removal efficiency of Cd(II) gradually increased at first, and reached a maximum value at 70 min, and then decreased slightly. For Pb(II) and Cu(II), the removal efficiencies showed a significant increase with the precipitation time varying from 10 to 30 min, after which it changed a little or declined narrowly. This was due to the hydroxy complexes and Fe(OH)$_3$ colloids hydrolyzed and polymerized from PFS could coagulate and settle the heavy metal ions. As the precipitation time prolonged, the heavy metals in the aqueous solution have almost settled completely, and if the coagulation time is too long, the coagulation already formed will be broken and the bridging adsorption capacity of the polymer chain will be reduced. Thus, the optimal precipitation times were selected at 70, 30, and 30 min for Cd(II), Pb(II), and Cu(II) removal, respectively.

3.2. Coagulation of combined heavy metals in DI water

3.2.1. Single-factor experiments

Actually, the target water samples may involve multiple heavy metals. Based on the single heavy metal coagulation experiments above, the parameter optimization
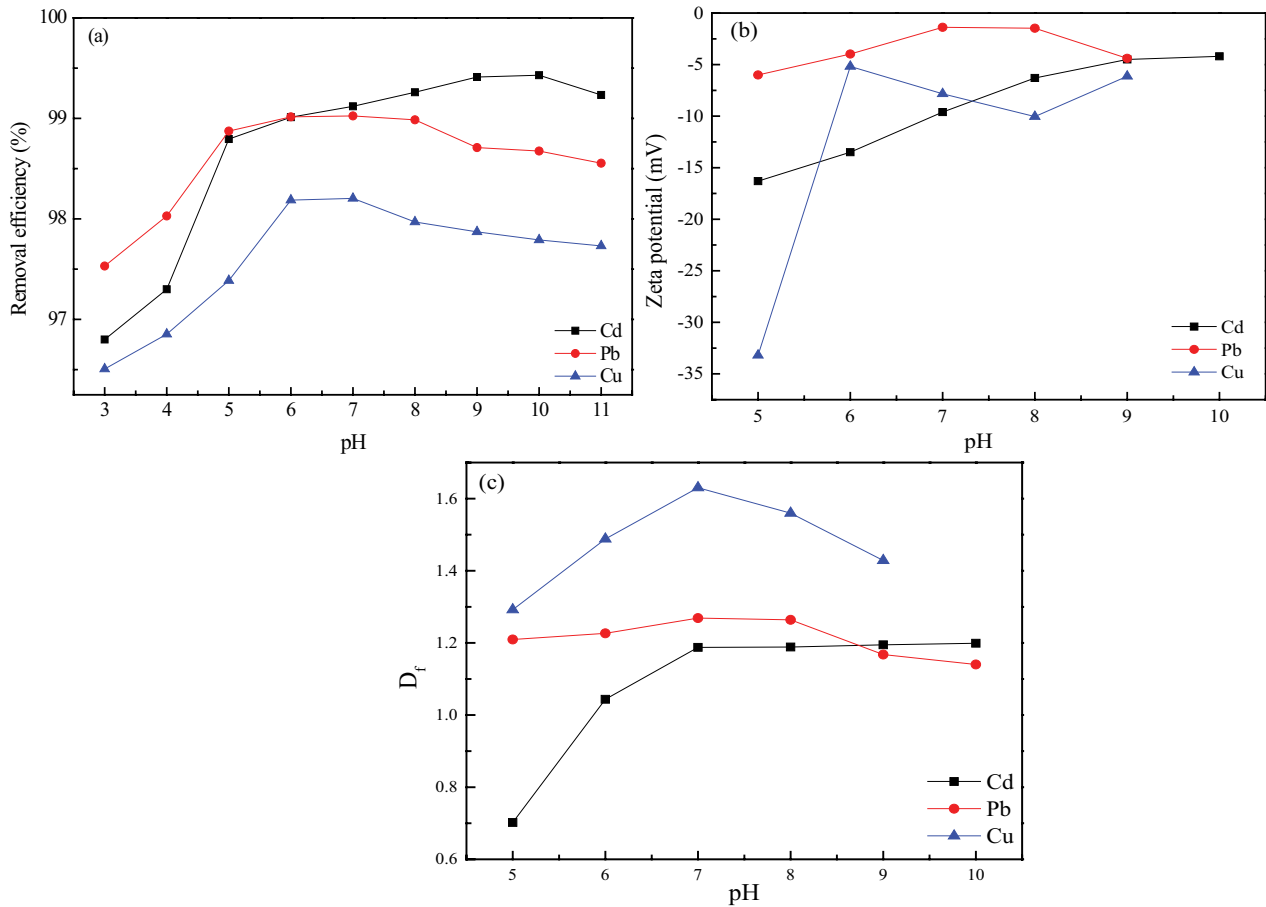
Fig. 2. Effect of pH on the coagulation of single heavy metals: (a) removal efficiencies, (b) zeta potential, and (c) fractal dimension.
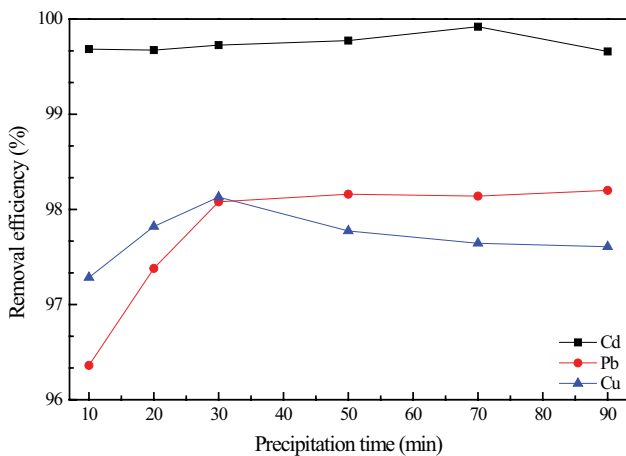

Fig. 3. Effect of precipitation time on the removal efficiency of single heavy metal.

experiments on the composite contaminated wastewater containing three kinds of most typical heavy metals were carried out (Fig. 4).

As shown in Fig. 4a, when the PFS dosage was closed to 60 mg/L, the three heavy metals could reach the "Integrated Wastewater Discharge Standard of China." At the same time,

the removal efficiency of the three heavy metals remained basically unchanged with further increase of PFS dosage. It could be inferred that when three heavy metals coexisted, Pb(II) and Cu(II) were prior to be coagulated and settled under a lower PFS dosage, and the removal effect of Cd(II) was getting better as the PFS dosage continuously increased.

Similarly, it can be seen from Fig. 4b that the removal efficiency of Pb(II) and Cu(II) was about 96%–97%, while that of Cd(II) was about 88%–92% under an acidic condition. When the pH was 6.0–7.0, the removal efficiencies of the three heavy metals were all over 98%, and the values declined slowly after the pH value was increased continually, indicating that the optimal pH range of coagulation precipitation in the presence of three heavy metals was 6.0–7.0. Fig. 4c depicts the influence of precipitation time on the coagulation of three metals, and it was found that when the treatment time was arranged from 30 to 50 min, appreciable removal efficiencies greater than 98% were obtained; once the coagulation time was too long, the flocs might be destroyed. Thus, the treatment effect was optimum when the precipitation time was about 30–50 min.

3.2.2. Response surface optimization experiment

In order to explore the optimal conditions for PFS coagulation treatment of composite heavy metal wastewater
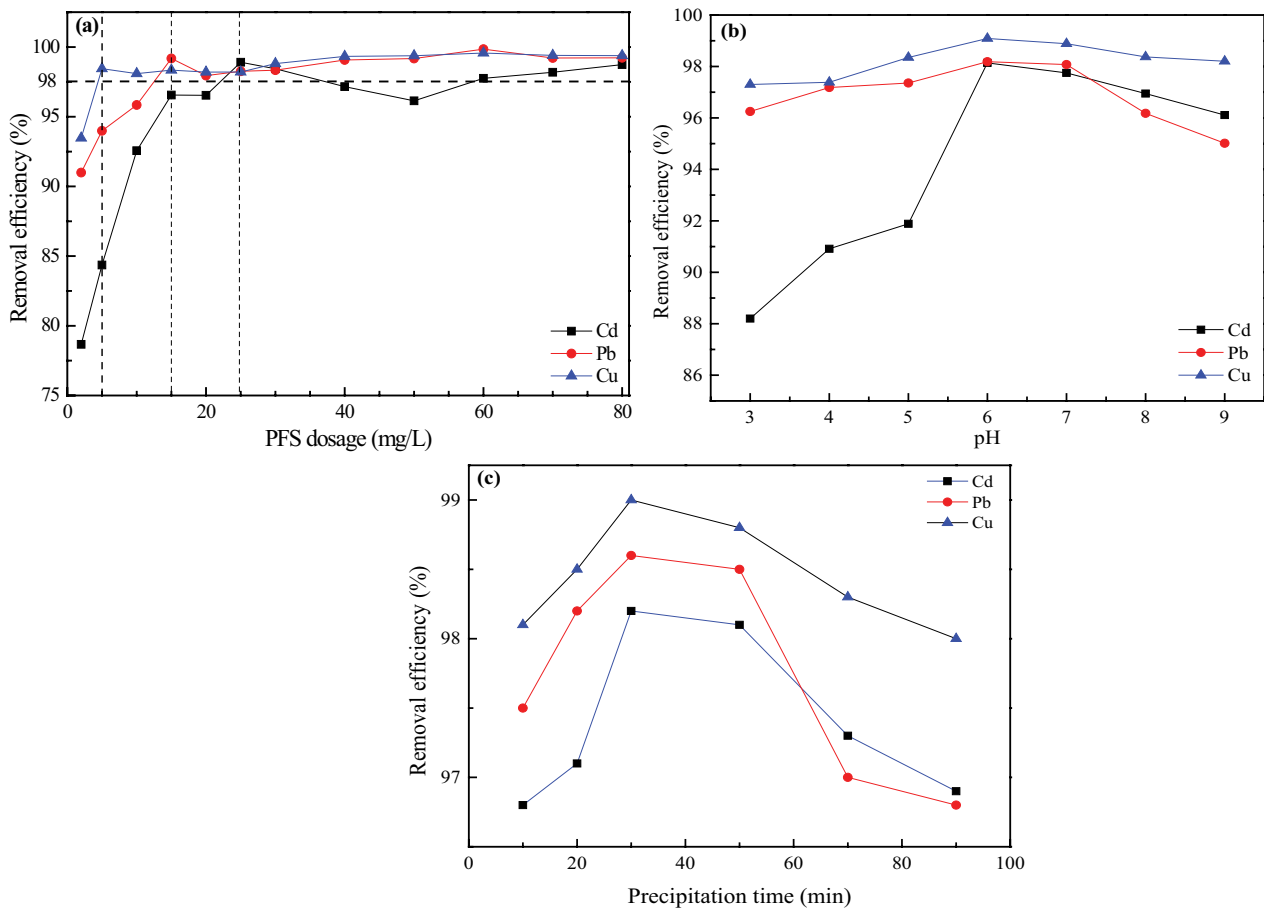
Fig. 4. Effect of (a) PFS dosage, (b) pH, and (c) precipitation time on removal efficiency of composite heavy metals.

more accurately, the response surface method was used for further optimization. Based on the factors and their levels indicated in Table 2, 17 experimental runs of enhanced coagulation using BBD were carried out, and the results are shown in Table 3.

A regression quadratic polynomial model was used to describe the relationship between the independent variables and the removal efficiency of heavy metals as shown in Eqs. (4)–(6).

$$Y_{Cd} = 98.13 + 8.973X_1 - 2.83X_2 + 0.37X_3 + 5.80X_1X_2 - 0.47X_1X_3 - 0.083X_2X_3 - 8.88X_1^2 - 4.42X_2^2 + 4.56X_3^2 \quad (4)$$

$$Y_{Pb} = 99.18 - 0.28X_1 - 0.079X_2 - 6.275E - 0.003X_3 - 0.046X_1X_2 + 0.4739X_1X_3 + 0.025X_2X_3 - 1.02X_1^2 - 0.64X_2^2 - 0.38X_3^2 \quad (5)$$

$$Y_{Cu} = 99.36 - 0.40X_1 - 0.31X_2 - 0.070X_3 + 0.24X_1X_2 - 0.10X_1X_3 + 0.10X_2X_3 - 0.99X_1^2 - 0.49X_2^2 - 0.43X_3^2 \quad (6)$$

where X_1, X_2, and X_3 are the variables including PFS dosage, pH, and precipitation time, respectively. Y_{Cd}, Y_{Pb}, and Y_{Zn} are the predicted responses for the removal efficiencies of Cd(II), Pb(II), and Cu(II), respectively. A p-value of less than 0.05 indicated that the significance of the model was acceptable.

If the p-value exceeded 0.01, the model would be considered insignificant as usual. More preferably, once the p-value was less than 0.0001, the fitted model was proved to be statistically significant.

The results of ANOVA for the removal of Cd(II), Pb(II), and Cu(II) are shown in Table 4. Fisher variation ratio (F-value) is a statistically effective measure to describe the variation of the means in the data. As shown in Tables 3, the F-values of the model were 14.78, 47.27, 19.54, and the p-values were 0.0257, 0.0001, and 0.0004, respectively, which indicated that the model was of high significance [31]. Obviously, the differences between the models in this study were within acceptable limits, which showed that the models fitted well with the actual situation and could be feasible for each response.

As tabulated in Table 4, the p-values of X_1, X_2, X_1X_2, and X_{12} were less than 0.05, indicating that the PFS dosage and pH affected the removal of Cd(II) significantly. Similarly, X_1, X_1X_2, X_1X_3, X_{12}, X_{22}, and X_{32} had a significant effect on the removal of Pb(II), and X_1, X_2, X_{12}, X_{22}, and X_{32} were the significant variables to remove Cu(II). It was known that the three independent variables had significant effects on the removal of the heavy metals with an order of PFS dosage > pH > precipitation time. Meanwhile, it can be inferred that the influence of different variables on the removal efficiency of heavy metals was not a pure linear relationship. The response

Table 3
Designed experiments and responses according to RSM

Runs	Factors			Responses			Experiment		
	PFS dosage (X_1)	pH (X_2)	Precipitation time (X_3)	Cd(II) removal (%)	Pb(II) removal (%)	Cu(II) removal (%)	ε-Cd(II)	ε-Pb(II)	ε-Cu(II)
1	−1	−1	0	83.18	98.06	98.87	0.041	0.019	0.025
2	1	−1	0	98.09	97.18	97.81	0.035	0.015	0.011
3	−1	1	0	59.99	97.76	97.48	0.012	0.028	0.032
4	1	1	0	98.10	97.07	97.36	0.050	0.031	0.022
5	−1	0	−1	87.90	98.35	98.45	0.018	0.035	0.041
6	1	0	−1	98.23	97.25	97.65	0.013	0.027	0.050
7	−1	0	1	90.34	97.52	98.44	0.027	0.049	0.017
8	1	0	1	98.80	97.97	97.23	0.034	0.014	0.039
9	0	−1	−1	98.08	98.22	98.73	0.029	0.027	0.041
10	0	1	−1	98.52	98.06	98.20	0.031	0.037	0.019
11	0	−1	1	98.20	98.20	98.46	0.047	0.019	0.042
12	0	1	1	98.31	98.14	98.35	0.019	0.028	0.025
13	0	0	0	98.03	99.07	99.16	0.028	0.017	0.017
14	0	0	0	98.10	99.25	99.45	0.037	0.039	0.041
15	0	0	0	99.19	99.11	99.28	0.019	0.043	0.037
16	0	0	0	98.18	99.23	99.44	0.028	0.021	0.029
17	0	0	0	98.17	99.24	99.46	0.042	0.018	0.026

Table 4
ANOVA results of the regression model for optimization of enhanced coagulation of the three heavy metals

Source	Sum of squares			D_f	F			Prob > F		
	Cd	Pb	Cu		Cd	Pb	Cu	Cd	Pb	Cu
Model	1,339	8.70	8.88	9	14.78	47.27	19.5	0.0257	<0.0001	0.0004
X_1	644.1	0.62	1.28	1	20.67	30.43	25.3	0.0026	0.0009	0.0015
X_2	64.11	0.05	0.77	1	2.06	2.46	15.2	0.1946	0.1608	0.0059
X_3	1.07	3.15×10^{-4}	0.04	1	0.034	0.015	0.79	0.8584	0.9047	0.4050
X_1X_2	134.58	8.41×10^{-3}	0.23	1	4.32	0.41	4.46	0.0463	0.5418	0.0725
X_1X_3	0.87	0.61	0.04	1	0.028	29.61	0.81	0.8717	0.0010	0.3973
X_2X_3	0.028	2.45×10^{-3}	0.04	1	8.80×10^{-4}	0.12	0.86	0.9771	0.7394	0.3853
X_{12}	331.85	4.41	4.11	1	10.65	215.69	81.4	0.0138	<0.0001	<0.0001
X_{22}	82.15	1.73	1.03	1	2.64	84.41	20.32	0.1484	<0.0001	0.0028
X_{32}	87.58	0.62	0.78	1	2.81	30.51	15.5	0.1375	0.0009	0.0056

surface plots and contour lines of the interaction effects of the variables on the objected responses are shown in Figs. 5–7.

3.2.2.1. Cd(II) removal

The slope of the response surface plots represented the significance of the variables on the responses. When the slope of the plots was steep, it showed a significant influence on the responses, otherwise the effect was not significant [32]. Besides, the shapes of the response surface can reflect the interaction between the variables. If the contour line was elliptical, the interaction was obvious, and once it was circular, there were unapparent interactions.

Fig. 5 shows the interaction between PFS dosage, pH value, and precipitation time on Cd(II) removal. As presented in Fig. 5a, the slope of the response surface was steep, indicating that there was a significant effect between PFS dosage and pH on the removal of Cd(II) ($p = 0.0463 < 0.05$), and its contour plots was elliptical, responding to an obvious interaction within the two variables. The surface plots had clear peaks, declaring that the optimum parameters for the maximum responses were in the range of the objected variables. When precipitation time was at 40 min, the Cd(II) removal efficiency increased and then decreased with the increasing PFS dosage and pH, reaching the maximum with the PFS dosage of 35 mg/L and initial pH of 6.0.
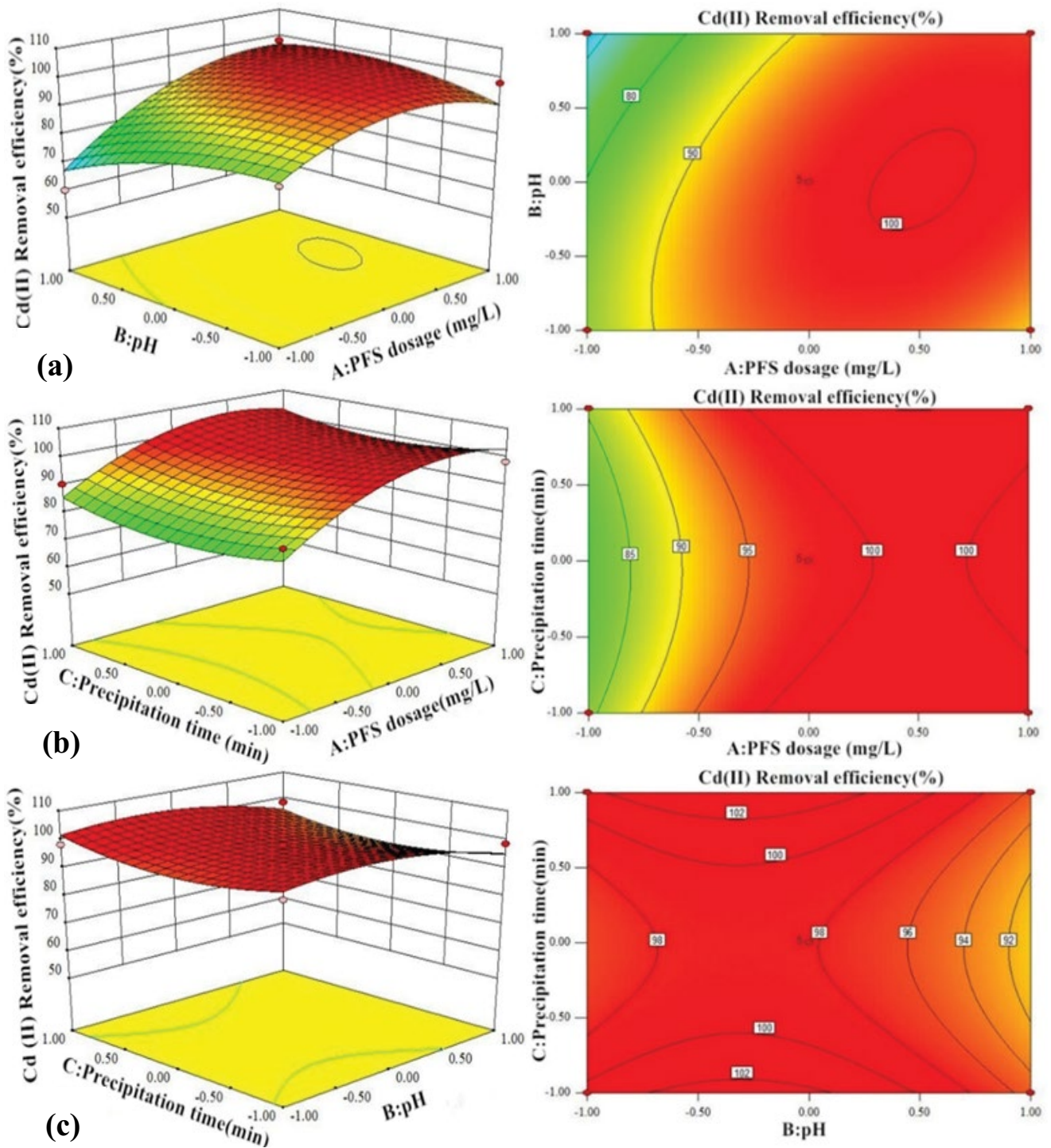
Fig. 5. Response surface for the removal efficiency of Cd(II) by PFS coagulation (a) the interaction between PFS dosage and pH, (b) the interaction between PFS dosage and precipitation time, and (c) the interaction between pH and precipitation time.

Fig. 5b shows the interaction of precipitation time and PFS dosage. The slope of the response surface of the precipitation time was flat, indicating that the precipitation time has no significant effect on the cadmium removal. In addition, the Cd(II) removal efficiency was gradually increased when the PFS dosage was increasing from 5 to 35 mg/L. However, an excessive PFS dosage had a suppressing effect on Cd(II) removal, which may be caused by the instability of colloids due to the excessive dosage. As seen from Fig. 5c, the interaction between precipitation time and pH on cadmium removal efficiency was not significant under the condition of a certain
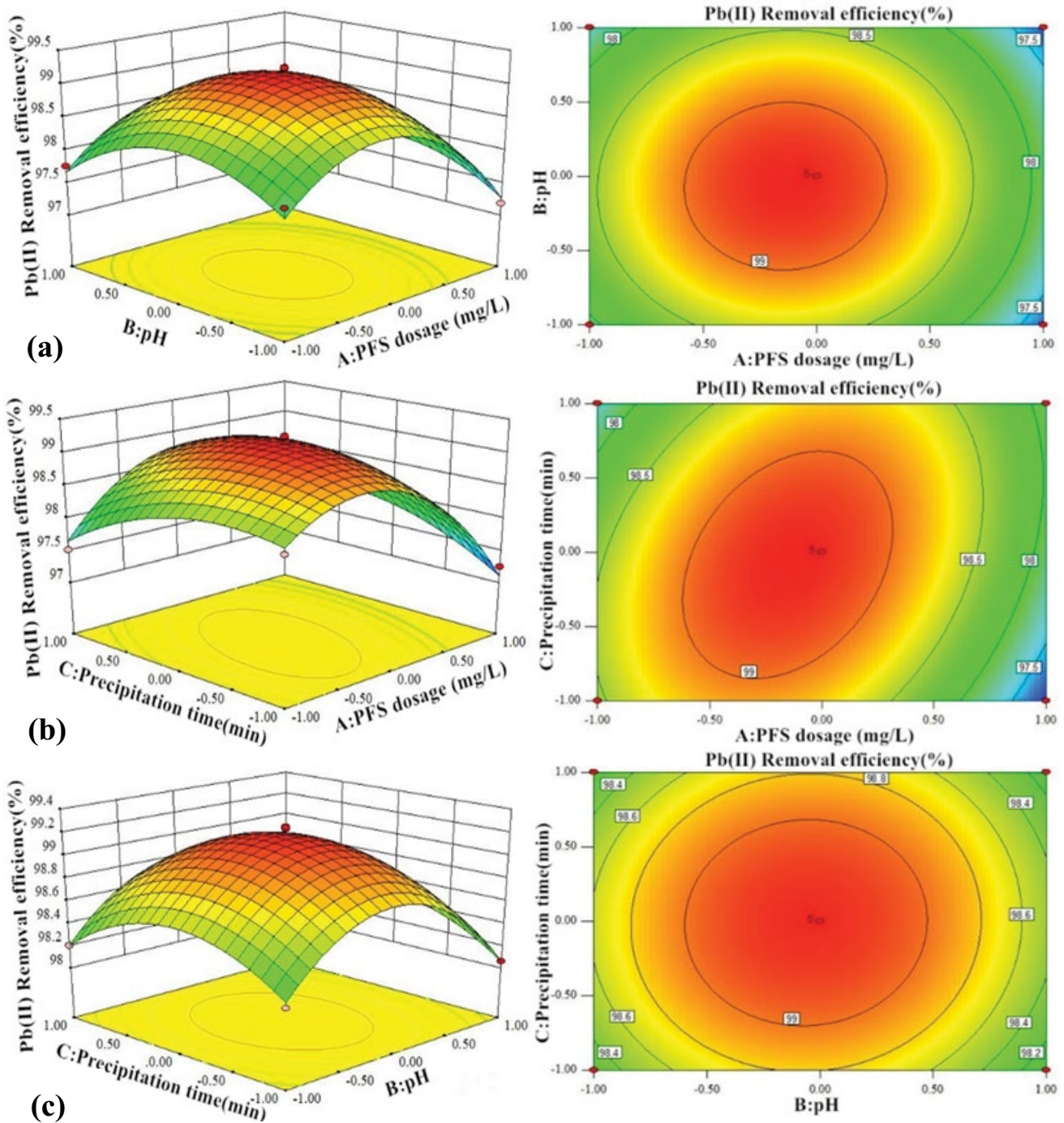
Fig. 6. Response surface for the removal efficiency of Pb(II) by PFS coagulation (a) the interaction between PFS dosage and pH, (b) the interaction between PFS dosage and precipitation time, and (c) the interaction between pH and precipitation time.

dosage. The precipitation time showed no obvious change in the response surface slope of cadmium removal, and the removal efficiency decreased when pH was greater than 6.0.

3.2.2.2. Pb(II) removal

Fig. 6 exhibits the influences of PFS dosage, pH and precipitation time on the output responses of removal efficiency of Pb(II). Significant interactions were observed between PFS dosage and pH, as well as between PFS dosage and precipitation time. As shown in Fig. 6a, the removal efficiency of Pb(II) was remarkably enhanced with reducing PFS dosage from 5 to 40 mg/L, especially under low neutral pH at 6.0–7.0. A feasible removal efficiency (>98%) was obtained with a PFS dosage of 20 mg/L at pH 6. PFS can be hydrolyzed to produce a highly cross-linked hydroxide
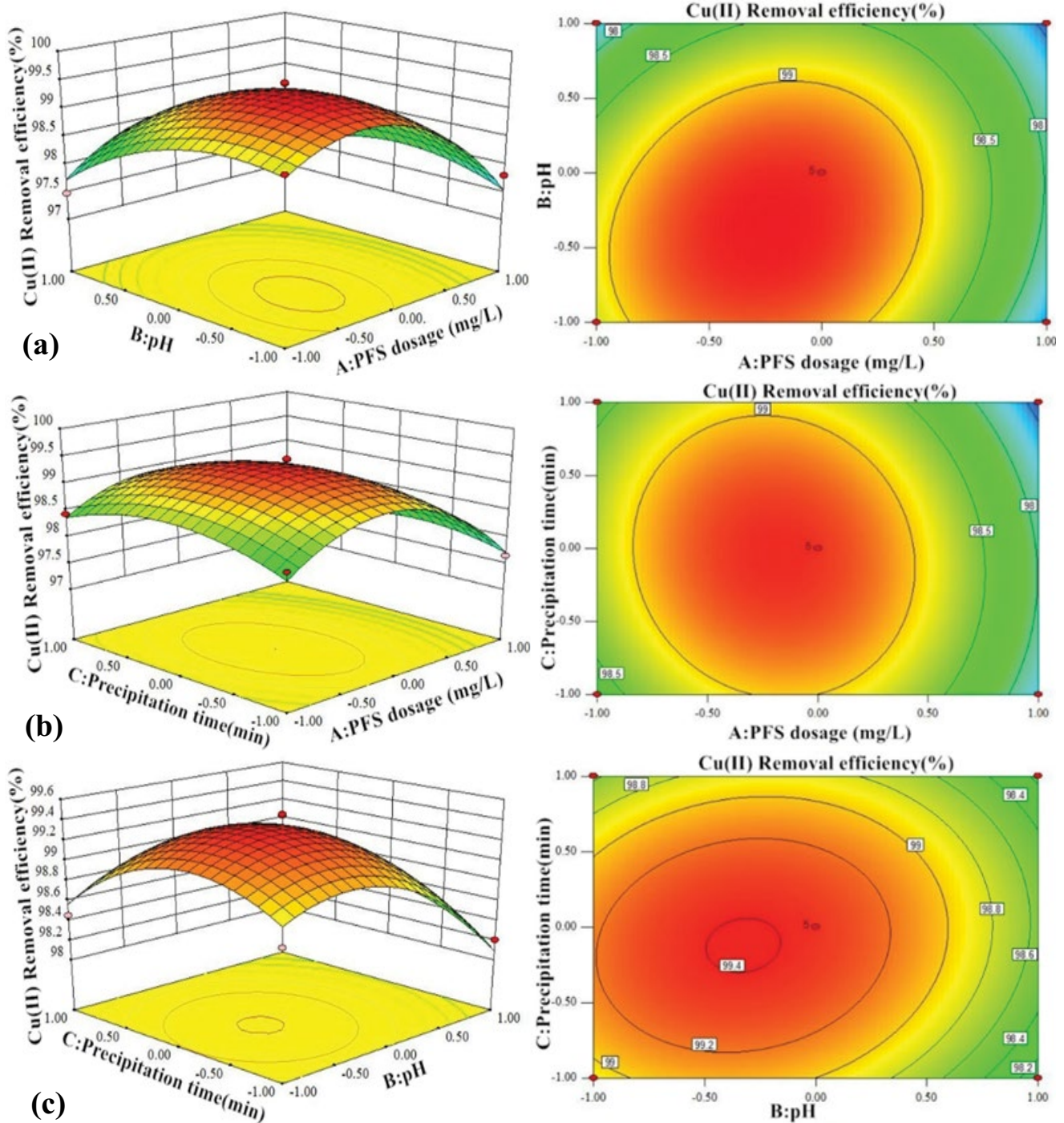
Fig. 7. Response surface for the removal efficiency of Cu(II) by PFS coagulation (a) the interaction between PFS dosage and pH, (b) the interaction between PFS dosage and precipitation time, and (c) the interaction between pH and precipitation time.

complex at a pH between 6.0 and 7.0, which was easier to capture, bridge, and entrap the positively charged lead ions. When the pH was further increased, the Pb(II) flocs would be reversed dissolved which meant a lower removal efficiency of Pb(II). Meanwhile, the slope of the response surface of pH and PFS dosage was steep, indicating that there was a strong interaction effect between these two variables on Pb(II) removal.

Fig. 6b shows the effect of PFS dosage and precipitation time on lead removal when the pH was at 6.0. It can be seen from the response surface plots that the slope of the surface of the precipitation time fluctuated with the increase of PFS dosage [33]. Highest removal efficiency was achieved when the dosage was 35 mg/L and the precipitation time was set at 40 min. Fig. 6c presents the interaction of the other two factors on the Pb(II) removal when the PFS dosage was

constant. Evidently, the slope of the response surface of both two factors was relatively flat, and the contour plots was almost circular, indicating an unobvious interaction between pH and precipitation time in the removal of Pb(II).

3.2.2.3. Cu(II) removal

Fig. 7 depicts the response surface of the interaction between PFS dosage, pH, and precipitation time on the Cu(II) removal efficiency. Fig. 7a shows a response surface plot where Cu(II) removal was represented by varying simultaneously PFS dosage from 5 to 65 mg/L and pH from 3.0 to 9.0. The removal efficiency was sensitive to the interaction between PFS dosage and pH which showed a synergistic influence on the variables. When the precipitation time was 40 min, the copper removal efficiency ascended initially and then decreased with the increase of pH, and the highest removal efficiency was achieved when pH was 6. This may due to the inhibition of the neutralization effect of the coagulant when pH was too high which would produce the negative ions and thus resulted in poor removal efficiency. Meanwhile, when the precipitation time was constant, the slope of the surface of the PFS dosage fluctuated with the change of pH, which illustrated a significant interaction between the two variables.

Fig. 7b shows the effect of precipitation time and PFS dosage on Cu(II) removal efficiency under certain pH values. The slope of the response surface of the PFS dosage had a violent fluctuation when the Cu(II) removal rate was not significantly affected by the precipitation time. It can be seen from Fig. 7c that the contour of the precipitation time and the pH were almost circular, indicating an insignificant interaction between them. When the PFS dosage was 35 mg/L and the pH was less than 6, the precipitation time played a minor role on the Cu(II) removal, and maximum efficiency was obtained after short-term precipitation.

Three sets of parallel experiments were carried out to determine an optimal required condition by constraining the values of PFS dosage, pH, and precipitation time, and thus found a maximum removal efficiency for each heavy metal, respectively. A desirable condition was achieved at the PFS dosage of 59.6 mg/L, the initial pH of 8.04, and the precipitation time of 45.4 min, with the Cd(II), Pb(II), and Cu(II) removal efficiency of 97.99%, 98.00%, and 98.01%, respectively. The validation experiments showed that the actual removal efficiency of 96.89%, 97.97%, and 98.12%, respectively, demonstrating a high coincidence between the regression prediction and the actual values. Thus, it was proved that the model obtained by BBD RSM can be used to find an optimal condition for the coagulation treatment.

3.2.3. Coagulation mechanism

In order to reveal the coagulation mechanism of the heavy metals, the XPS spectra of heavy metal ions in flocs under the optimal coagulation conditions selected after precipitation are recorded in Fig. 8. The Cd 3d spectra including $3d^{5/2}$ and $3d^{3/2}$ with the binding energies of
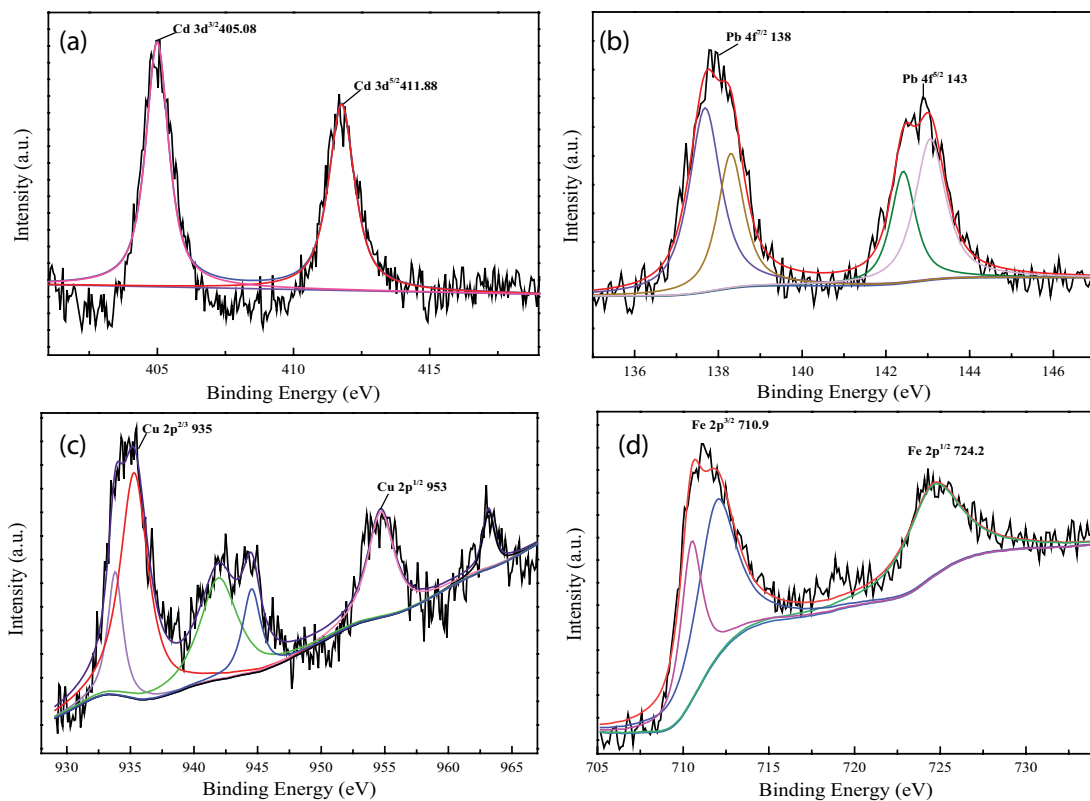

Fig. 8. Chemical state of elements of flocs after flocculation (a) Cd(II), (b) Pb(II), (c) Cu(II), and (d) Fe(III).

405.08 and 411.88 eV were found, which can be attributed to the generation of Cd(OH)$_2$, CdCO$_3$, or other Cd polymers. The Pb 4f$^{7/2}$ and Pb 4f$^{5/2}$ peaks were observed at 138.0 and 143.0 eV, respectively, while the former could be classified as (Pb$_2$(OH)$_2$(CO$_3$)$_2$), demonstrating that the mechanism of the coagulation process was mainly in electric neutralization and purge coagulation. As shown in Fig. 8, the curve fitting of the Cu 2p$^{2/3}$ signal was divided into two peaks, with the binding energy of 934.08 and 935.28 eV, and the former can could be classified as Cu(II) signal. In addition, the oxidized state structure of Cu could be identified from the strong satellite features appearing at 943 eV and 962 eV. The XPS spectra of 724.2 eV Fe 2p$^{1/2}$ and 710.9 eV Fe 2p$^{3/2}$ in the compound floc were consistent with the electron peak of Fe(III). The Fe(III) ion can be hydrolyzed in an aqueous solution to form a hydroxide, which promotes destabilization and agglomeration of the colloidal particles, thereby achieving the coagulation and sedimentation.

Moreover, the SEM images of the flocs after coagulation indicated that when PFS amount was too low to provide sufficient coordination charge, the compression of double-layer would occur, resulting in loose floc structure and small D_f; when the dosage of PFS increased to a proper range, more coordinated charges were produced, which promoted the electric neutralization and the bridging between particles, leading to the dense flocs. However, when the PFS dosage was too large, the flocs become loose, even forming holes that were prone to rupture. Similarly, the change in pH affected the hydrolysis of PFS. With the increase of the pH, the hydrolysis of PFS was promoted, and a more effective iron hydroxyl complex was formed, leading to stronger and tighter flocs. Then, the best removal efficiency was obtained. However, when the pH value exceeds a certain range, the polymer was partially dissolved, and the apparent lower flocculate density and looser surface structure in SEM morphology could be explained. The SEM images of the flocs under the optimal coagulation conditions are shown in Fig. 9.

3.3. Coagulation of combined heavy metals in real wastewater

The coagulation experiments were carried out in real wastewater containing the above heavy metals including Cd(II), Pb(II), and Cu(II), and the PFS dosage was optimized. The initial pH of the water sample was adjusted to set at 8.0 ± 0.1 and the precipitation time was set at 45.4 min, which was consistent with the optimal conditions described above. As shown in Fig. 10, when the PFS dosage was close to 60 mg/L, the removal rates of all the three heavy metals were more than 98%, and the remaining concentrations can reach the requirement of the "Integrated Wastewater Discharge Standard of China." The removal efficiency of the three heavy metals remained basically unchanged with the further increase of PFS dosage. The curves of zeta potential and D_f fractal dimension are basically consistent with the removal rate curve.
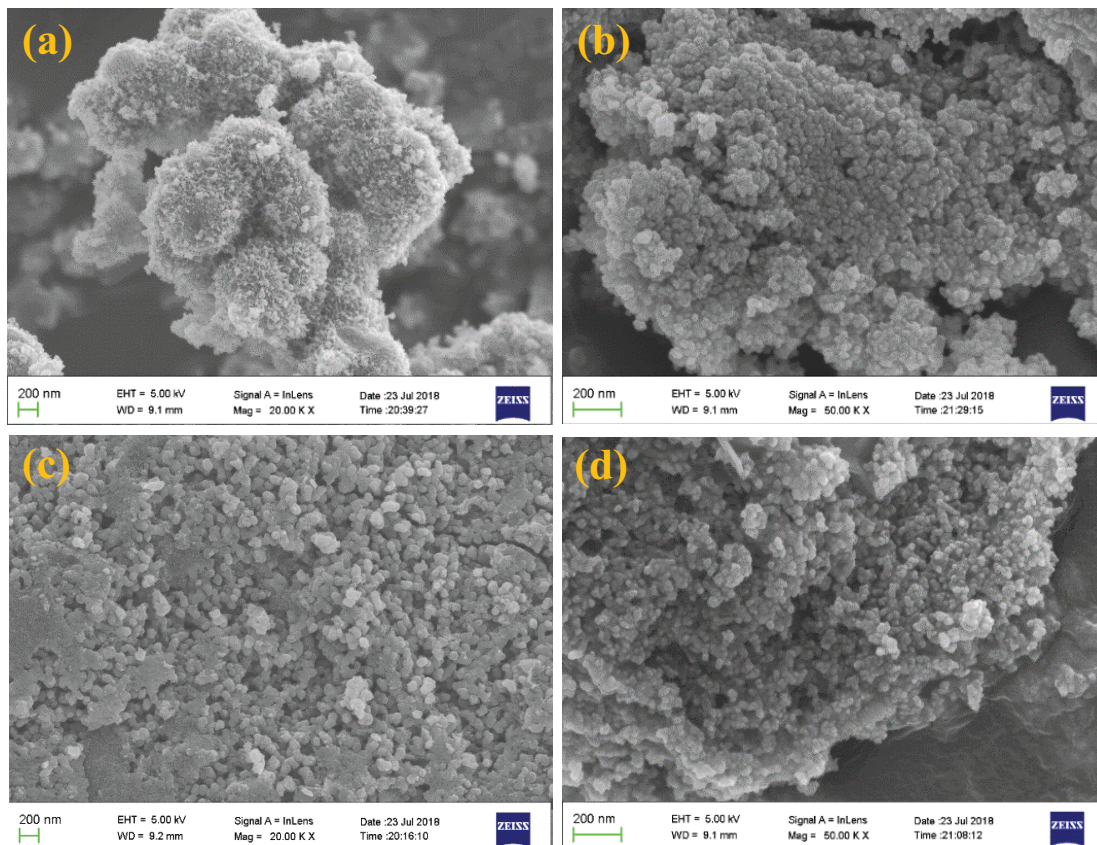

Fig. 9. SEM images of the flocs after flocculation (a) Cd(II), (b) Pb(II), (c) Cu(II), and (d) Fe(III).
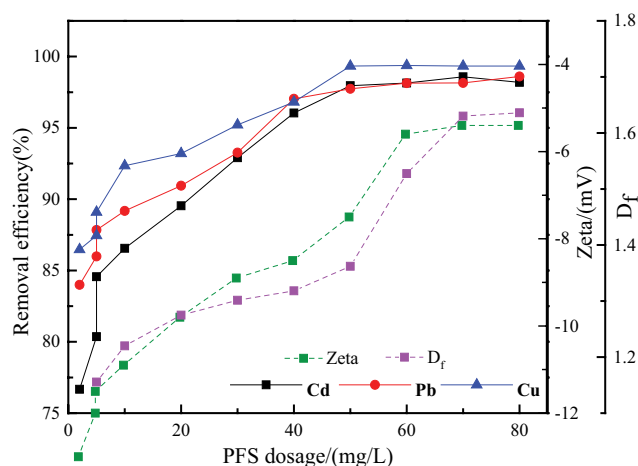
Fig. 10. Effect of PFS dosage on heavy metals removal efficiencies, Zeta potential of the water, and D_f of the flocs.

4. Conclusions

In this paper, PFS was used to coagulate combined heavy metals in water, and coagulation parameters were optimized. The results of single-factor coagulation experiments show that the optimal conditions for Cd(II), Pb(II), and Cu(II) with the concentration of 5, 50, and 25 mg/L, respectively, were PFS dosage 30, 15, and 3 mg/L, pH 9,0–10.0, 6.0–8.0, and 6.0–7.0, and precipitation time 70, 30, and 30 min. Meanwhile, the maximum removal efficiency of the combined wastewater was obtained at PFS dosage 60 mg/L, pH 6.0–7.0, and precipitation time 30–50 min. The PFS dosage, pH, and precipitation time were selected as independent variables, while the removal efficiencies of three heavy metals were considered as the response values, and second-order polynomial equations (regression models) were thus established which was well fitted to the experimental data. Based on the ANOVA analysis in RSM experiments, pH and PFS dosage were found to be the most significant parameters in the coagulation of three metals, which exhibited a positive effect on the responses. According to the RSM optimization perform, the optimum condition for coagulation in the combined wastewater with the concentration of Cd(II), Pb(II), and Cu(II) of 5, 50, and 25 mg/L, respectively, was PFS dosage 59.6 mg/L, pH 8.04, precipitation time 45.4 min, respectively. It was confirmed that under the optimal conditions, the coagulated effluent of the real combined wastewater could also meet the standard above. Meanwhile, the zeta potential of the supernatant and the fractal dimension (D_f) of the flocs after precipitation under the optimal coagulation conditions were measured to illustrate the consistency of the removal efficiency of heavy metals with the trend of zeta potential and fractal dimension. According to the XPS analysis, it can be referred that electric neutralization and purge coagulation played a relatively dominant role during coagulation.

Acknowledgments

References

[1] T.Y. Hou, H.W. Du, Z.Q. Yang, Z. Tian, S.C. Shen, Y.X. Shi, W.B. Yang, L.M. Zhang, Coagulation of different types of combined contaminants of antibiotics and heavy metals by thermo-responsive flocculants with various architectures, Sep. Purif. Technol., 223 (2019) 123–132.

[2] F. Fu, Q. Wang, Removal of heavy metal ions from wastewaters: a review, J. Environ. Manage., 92(2011) 407–418.

[3] A. Karbassi, A. Marefat, The impact of increased oxygen conditions on heavy metal coagulation in the Sefidrud estuary, Mar. Pollut. Bull., 121(2017) 168–175.

[4] S.Yu. Bratskaya, A.V. Pestov, Yu.G. Yatluk, V.A. Avramenko, Heavy metals removal by coagulation/precipitation using *N*-(2-carboxyethyl) chitosans, Colloid Surf., A, 339(2009) 140–144.

[5] H.A. Aziz, M.N. Adlan, K.S. Ariffin, Heavy metals (Cd(II), Pb(II), Zn(II), Ni(II), Cu(II) and Cr(III) removal from water in Malaysia: post treatment by high quality limestone, Bioresource. Technol., 99 (2018) 1578–1583.

[6] N.N. Nassar, Rapid removal and recovery of Pb(II) from wastewater by magnetic nanoadsorbents, J. Hazard. Mater., 184 (2010) 538–46.

[7] S. Yılmaz, A. Zengin, Y. Akbulut, T. Sahan, Magnetic nanoparticles coated with aminated polymer brush as a novel material for effective removal of Pb(II) ions from aqueous environments, J. Environ. Sci. Pollut. Res., 26 (2019) 20454–20468.

[8] M.G. Yu, Y.X. Chen, Biosorption of heavy metals from solution by tea waste: a review, J. Appl. Ecol., 21 (2010) 505–513.

[9] Z. Jin, S. Deng, Y. Wen, Y. Jin, L. Pan, Y. Zhang, T. Black, K.C. Jones, H. Zhang, D. Zhang, Application of Simplicillium chinense for Cd(II) and Pb(II) biosorption and enhancing heavy metal phytoremediation of soils, Sci. Total Environ., 697 (2019) 134–148.

[10] F.R. Espinoza-Quiñones, A.N. Módenes, P.S. Theodoro, S.M. Palácio, D.E.G. Trigueros, C.E. Borba, M.M. Abugderah, A.D. Kroumov, Optimization of the iron electro-coagulation process of Cr, Ni, Cu, and Zn galvanization by-products by using response surface methodology, Sep. Sci. Technol., 47 (2018) 688–699.

[11] L. Cai, L. Cui, B. Lin, J. Zhang, Z. Huang, Advanced treatment of piggery tail water by dual coagulation with Na⁺ zeolite and Mg/Fe chloride and resource utilization of the coagulation sludge for efficient decontamination of Cd(II), J. Cleaner Prod., 202 (2018) 759–769.

[12] V. Orescanin, D. Tibljas, V. Valkovic, A study of coagulant production from red mud and its use for heavy metals removal, J. Trace Microprobe Tech., 20 (2002) 233–245.

[13] Q. Imran, M. Hanif, M. Riaz, S. Noureen, T. Ansari, H. Bhatti, Coagulation/coagulation of tannery wastewater using immobilized chemical coagulants. J. Appl. Res. Technol., 10 (2012) 79–86.

[14] A. Matilainen, M. Vepsäläinen, M. Sillanpää, Natural organic matter removal by coagulation during drinking water treatment: a review, Adv. Colloid Interface Sci., 159 (2010) 189–97.

[15] I.A. Katsoyiannis, N.M. Tzollas, A.K. Tolkou, M. Mitrakas, M. Ernst, A.I. Zouboulis, Use of novel composite coagulants for arsenic removal from waters-experimental insight for the application of polyferric sulfate (PFS), Sustainability, 197 (2017) 9–16.

[16] I. Khouni, B. Marrot, P. Moulin, R.B. Amar, Decolourization of the reconstituted textile effluent by different process treatments: enzymatic catalysis, coagulation/coagulation and nanofiltration processes, Desalination, 268 (2011) 27–37.

[17] C.Y. Teh, P.M. Budiman, K.P.Y. Shak, T.Y. Wu, Recent advancement of coagulation–coagulation and its application in wastewater treatment, Ind. Eng. Chem. Res., 55 (2016) 109–118.

[18] S. Zhao, Z. Chen, J. Shen, J. Kang, Y. Qu, B. Wang, X. Wang, L. Yuan, Response surface methodology investigation into

optimization of the removal condition and mechanism of Cr(VI) by Na₂SO₃/CaO, J. Environ. Manage., 202 (2017) 38–45.

[19] K. Wantala, E. Khongkasem, N. Khlongkarnpanich, S. Sthiannopkao, K.W. Kim, Optimization of As(V) adsorption on Fe–RH–MCM-41-immobilized GAC using Box–Behnken design: effects of pH, loadings, and initial concentrations, Appl. Geochem., 27 (2013) 1027–1034.

[20] M. Saad, H. Tahir, Synthesis of carbon loaded γ-Fe₂O₃ nanocomposite and their applicability for the selective removal of binary mixture of dyes by ultrasonic adsorption based on response surface methodology, Ultrason. Sonochem., 36 (2017) 393–408.

[21] H. Trinh, H.T. Duong, T.T. Ta, C.H. Van, B.W. Strobel, G.T. Le, Simultaneous effect of dissolved organic carbon, surfactant and organic acid on the desorption of pesticides investigated by response surface methodology, Environ. Sci. Pollut. Res. Int., 24 (2017) 38–43.

[22] S. Yılmaz, U. Ecer, T. Sahan, Modelling and optimization of As(III) adsorption onto thiol-functionalized bentonite from aqueous solutions using response surface methodology approach, ChemistrySelect, 3 (2018) 9326–9335.

[23] N. Rahman, M. Nasir, Application of Box–Behnken design and desirability function in the optimization of Cd(II) removal from aqueous solution using poly(o-phenylenediamine)/hydrous zirconium oxide composite: equilibrium modeling, kinetic and thermodynamic studies, Environ. Sci. Pollut. Res. Int., 36 (2018) 11–21.

[24] Y. Zheng, A. Wang, Removal of heavy metals using polyvinyl alcohol semi-IPN poly (acrylic acid)/tourmaline composite optimized with response surface methodology, Chem. Eng. J., 162 (2010) 186–193.

[25] M. Askari, E. Salehi, M. Ebrahimi, A. Barati, Application of breakthrough curve analysis and response surface methodology for optimization of a hybrid separation system consisting of fixed-bed column adsorption and dead-end depth filtration, Chem. Eng. Process, 143 (2019) 107594.

[26] M. Iqbal, N. Iqbal, I.A. Bhatti, N. Ahmad, M. Zahid, Response surface methodology application in optimization of cadmium adsorption by shoe waste: a good option of waste mitigation by waste, Ecol. Eng., 88 (2016) 265–275.

[27] R.B. Moruzzi, A.L. De Oliveira, C.F. Da, J. Gregory, L.C. Campos, Fractal dimension of large aggregates under different coagulation conditions, Sci. Total Environ., 9 (2017) 807–814.

[28] A.J. Bora, R.K. Dutta, Removal of metals (Pb, Cd, Cu, Cr, Ni, and Co) from drinking water by oxidation–coagulation–absorption at optimized pH, J. Water Process Eng., 31 (2019) 100839.

[29] M. Fan, C. Nie, H. Du, J. Ni, An insight into the solar demulsification of highly emulsified water produced from oilfields by monitoring the viscosity, zeta potential, particle size and rheology, Colloids Surf., A, 575 (2019) 144–154.

[30] Y. Cui, J. Li, A. Chen, J. Wu, Fractal dimensions and morphological characteristics of aggregates formed in different physico-chemical and mechanical coagulation environments, Catena, 180 (2019) 252–262.

[31] K.P.Y. Shak, T.Y. Wu, Coagulation–coagulation treatment of high-strength agro-industrial wastewater using natural Cassia obtusifolia seed gum: treatment efficiencies and flocs characterization, Chem. Eng. J., 256 (2014) 293–305.

[32] A. Fathianpour, M. Taheriyoun, M. Soleimani, Lead and zinc stabilization of soil using sewage sludge biochar: optimization through response surface methodology, Clean Soil Air Water, 23 (2019) 108–119.

[33] V.V. Arun, N. Saharan, V. Ramasubramanian, A.M. Babitha Rani, K.R. Salin, R. Sontakke, H. Haridas, D.G. Pazhayamadom, Multi-response optimization of Artemia hatching process using split-split-plot design based response surface methodology, Sci. Rep., 7 (2017) 403–414.